

# INCOMPRESSIBLE SMOOTHED PARTICLE HYDRODYNAMICS (ISPH) MODELLING OF BREAKWATER OVERTOPPING

Benedict D. Rogers<sup>1</sup>, Maël Morellec<sup>2</sup>, Peter K. Stansby<sup>1</sup>, Alex Skillen<sup>1</sup>

This paper describes an investigation into using incompressible smoothed particle hydrodynamics (ISPH) to simulate the overtopping of a coastal structure such as a breakwater. The paper presents the ISPH formulation that employs the multiple boundary tangent method and the latest developments such as particle shifting that produce noise-free pressure fields. The numerical model is compared with experimental overtopping data for a solitary wave and a crest-focussed wave group approaching a trapezoidal breakwater. The ISPH model is shown to produce close agreement for the free-surface evolution for both types of wave and generates overtopping volumes in satisfactory agreement with experimental data. Closer agreement with experimental data is obtained for ISPH compared to more popular weakly compressible SPH for the same resolution or particle size. Future work identifies conducting a convergence study and using more sophisticated boundary treatments.

*Keywords: overtopping; incompressible smoothed particle hydrodynamics; SPH; ISPH; breakwater*

## INTRODUCTION

At present, engineers possess mainly empirical means to predict the overtopping of coastal protection structures. The modelling and simulation of such highly nonlinear and potentially violent free-surface motion is an extremely challenging task with numerous difficulties. In this work, we examine the behaviour of violent wave overtopping processes using truly incompressible smoothed particle hydrodynamics (SPH).

SPH describes a fluid by replacing its continuum properties with locally smoothed quantities at discrete Lagrangian locations. Thus, the domain can be multiply-connected with no special treatment of the free surface, making it ideal for examining complicated flow situations.

SPH has become increasingly popular in recent years as a novel technique to model the violent hydrodynamics in wave breaking, etc. (Rogers and Darlymple 2006). However, the vast majority of SPH schemes are based on the weakly compressible SPH (WCSPH) formulation where the density is allowed to vary slightly so that compressibility effects are kept within 1%. This is generally acceptable for engineering computations (Rogers *et al.* 2010), but can lead to severe problems when predicting impact pressures while the propagation of waves can exhibit significant decay and dissipation.

In Manchester, we have been developing a truly incompressible SPH (ISPH) scheme where a pressure Poisson equation is solved to predict pressure fields. A novel shifting algorithm has effectively eliminated unphysical diffusion at the free-surface leading to accurate noise-free pressure fields for a range of test cases including periodic waves, impulsively moving plates, and slam problems (Lind *et al.* 2012, Skillen *et al.* 2013). For the simulation of overtopping, previous work using the weakly compressible approach (Stansby *et al.* 2008) produced close agreement with experimental data for solitary waves. The application of ISPH to overtopping is the next important step in the development of this method.

In this paper, first we introduce the SPH discretisation. This includes a short description of the methodology for enforcing strict incompressibility within SPH. The next section presents the numerical results for two cases of a solitary wave and a crest-focussed wave group overtopping a breakwater. Comparisons with experimental data for overtopping the breakwater are presented.

## INCOMPRESSIBLE SPH MODEL

### SPH Methodology

Smoothed Particle Hydrodynamics (SPH) is based on the approximate representation of continuous interpolations or integrals by a discrete particle representation. The value of a flow quantity,  $\phi$ , at a position vector  $\mathbf{r}$  is approximated by a local summation

---

<sup>1</sup> School of Mechanical, Civil and Aerospace Engineering, University of Manchester, Manchester, M13 9PL, UK

<sup>2</sup> Enseignement Supérieur à l'Ecole Normale Supérieure de Cachan, France

$$\langle \phi(\mathbf{r}) \rangle = \sum_j \phi_j \omega(\mathbf{r} - \mathbf{r}_j) V_j, \quad (1)$$

where  $V_j$  is the volume of the  $j$ th particle located at  $\mathbf{r}_j$  with scalar quantity  $\phi_j$ , and  $\omega(\mathbf{r} - \mathbf{r}_j)$  is the weighting function called the smoothing kernel. The kernel is specified prior to simulation by an analytical expression making its computation straightforward. In all results presented, a fifth-order spline kernel has been used (Lind *et al.* 2012). The kernel has a characteristic smoothing length,  $h$ , which defines the region of influence, and is preset to be  $1.3\Delta x$  for the duration of all simulations where  $\Delta x$  is the initial particle spacing.

In SPH function derivatives can be expressed as another summation by simply using a derivative of the smoothing kernel, i.e.

$$\frac{\partial f(\mathbf{r}_i)}{\partial x_i} = \sum_j (f_j - f_i) \frac{\partial W_{ij}(\mathbf{r}_i - \mathbf{r}_j)}{\partial x_i} V_j. \quad (2)$$

where  $W_{ij} = W(\mathbf{r}_i - \mathbf{r}_j)$ . This avoids complicated expressions for calculating derivatives since an analytical expression is known for the specified kernel. Expression (2) also ensures that there is zero divergence for a uniformly constant field.

### Governing Equations

Herein, we solve the incompressible Navier-Stokes equations in Lagrangian form such that the divergence of the velocity field is zero  $\nabla \cdot \mathbf{u} = 0$  where  $\mathbf{u}$  is the velocity. The conservation of momentum is therefore written as:

$$\frac{d\mathbf{u}}{dt} = -\frac{1}{\rho} \nabla P + \nu \nabla^2 \mathbf{u} + \mathbf{g} \quad (3)$$

where  $P$  is pressure,  $\rho$  is density,  $\nu$  is viscosity,  $t$  is time and  $\mathbf{g}$  is gravity. Incompressibility is enforced using a pressure Poisson equation. Using a fractional step method, the pressure gradient term is discretized according to:

$$-\frac{1}{\rho} \nabla P_i = -\frac{1}{\rho} \sum_j V_j (P_j - P_i) \nabla_i W_{ij} \quad (4)$$

where  $W$  represents the corrected kernel gradient as used by Lind *et al.* (2012). The viscous and gravity terms are discretised as

$$\nu \nabla^2 \mathbf{u} + \mathbf{g} = \sum_j V_j \frac{2\nu \mathbf{r}_{ij} \cdot \nabla_i \omega_{ij}}{(r_{ij} + 0.01h^2)} \mathbf{u}_{ij} + \mathbf{g}. \quad (5)$$

### Pressure Projection Method

The solution of the pressure gradient term follows the approach first suggested by Cummins and Rudman (1999) for SPH. To solve Eq. (3), the solution first advects the particles to an intermediate location

$$\mathbf{r}_i^* = \mathbf{r}_i^n + \Delta t \mathbf{u}_i^n \quad (6)$$

An intermediate velocity,  $\mathbf{u}_i^*$ , based on viscosity and body forces is then computed

$$\mathbf{u}_i^* = \mathbf{u}_i^n + (\nu \nabla^2 \mathbf{u}_i^n + \mathbf{g}) \Delta t \quad (7)$$

The pressure at time level  $n+1$  is computed from the Pressure Poisson equation

$$\nabla \cdot \left( \frac{1}{\rho} \nabla P_i^n \right) = \frac{1}{\Delta t} \nabla \cdot \mathbf{u}_i^* \quad (8)$$

This produces a matrix equation which is solved using a Bi-CGSTAB method. (van der Vorst 1992). This enables the projection of  $\mathbf{u}_i^*$  onto the divergence-free space giving the velocity at time  $n+1$ :

$$\mathbf{u}_i^{n+1} = \mathbf{u}_i^* - \frac{\Delta t}{\rho} \nabla P_i^{n+1} \quad (9)$$

The particles' positions are then updated using a centred time integration scheme

$$\mathbf{r}_i^{n+1} = \mathbf{r}_i^n + \Delta t \left( \frac{\mathbf{u}_i^{n+1} + \mathbf{u}_i^n}{2} \right) \quad (10)$$

### Particle Shifting

The pressure projection approach of Cummins and Rudman (1999) has been shown to be unstable for irregular particle distributions (Xu *et al.* 2009). Lind *et al.* (2012) and Skillen *et al.* (2013) have shown that noise-free pressure fields for free-surface flow can be computed by shifting particles a small distance  $\delta \mathbf{r}_i$  according to the gradient of the local concentration of the particles  $C$ :

$$\delta \mathbf{r}_i = -D \nabla C_i \quad (11)$$

where  $D$  is a local diffusion coefficient. The diffusion coefficient is a numerical parameter evaluated according to the maximum timestep:

$$D = \frac{0.5h^2}{\Delta t_{\max}} \quad (12)$$

where  $\Delta t_{\max}$  is provided by a CFL condition:

$$\Delta t_{\max} \leq 0.1 \frac{h}{U_{\max}} \quad (13)$$

where  $U_{\max}$  is the maximum particle velocity. In order to prevent the particles being shifted either beyond or too close to each other, the shifting distance,  $\delta \mathbf{r}_i$ , is restricted to a maximum value of  $0.2h$ .

A measure of the particle concentration can be computed from the sum of the kernel function:

$$C_i = \sum_j \omega_{ij} V_j \quad (14)$$

So the gradient of the concentration is given by

$$\nabla C_i = \sum_j V_j (1 + f_{ij}) \omega_{ij} \quad (15)$$

where  $f_{ab}$  is a tensile correction term (Lind *et al.* 2012). The hydrodynamic variables are finally corrected by a Taylor series approximation.

### Boundary Treatment

The original SPH method does not include the presence of boundaries naturally since the particle approximation in Eq. (1) is only a volume integral and does not account for the missing kernel support in the vicinity of boundaries. There have been many different treatments for boundaries proposed in SPH (see Ferrand *et al.* 2012 for a comparison of some popular methods). In this work, we use the multiple boundary tangent (MBT) method of Yildiz *et al.* (2009). In the MBT approach, a fluid particle will interact with a wall particle,  $w_i$ . A tangent at  $w_i$  is computed and then a localized mirror image of the fluid particles is generated using that tangent line as shown in Fig. 1 for different cases. For overlapping mirror images, the mass of each particle is adjusted so as to maintain a physical correct volume.

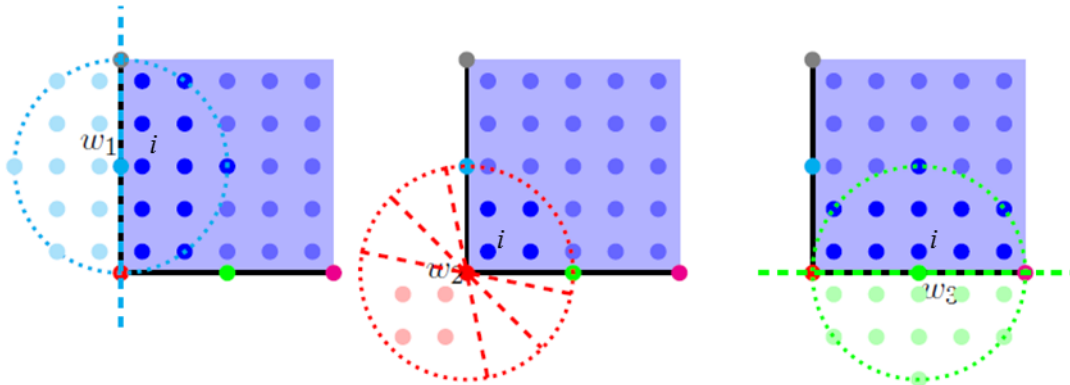


Figure 1 Multiple boundary tangent (MBT) method (Yildiz *et al.* 2009) for generating localised mirror images for different cases

## NUMERICAL RESULTS

Hunt Raby *et al.* (2011) conducted experiments measuring wave-by-wave overtopping of a trapezoidal structure for both solitary waves and focused wave groups. Based on these experiments, the geometry for the ISPH simulations is shown in Fig. 2 where the water is of depth 0.5 m and the particle size or resolution is 0.01 m. A paddle at the left-hand side generates waves that propagate over the beach towards the trapezoidal structure.

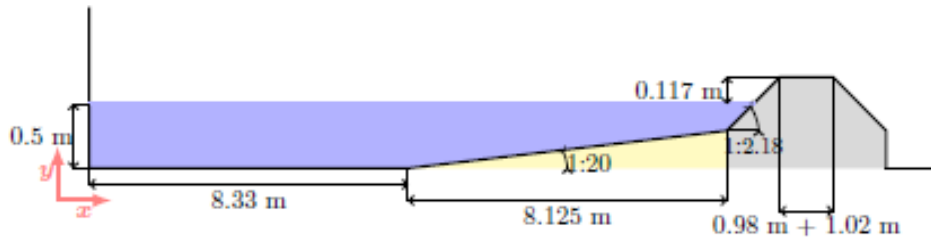


Figure 2 Geometry for UKCRF experiments and ISPH simulations

### Solitary Wave Overtopping

In Fig. 3, we can see a comparison for the free surface at different time instants with (a) a Boussinesq-type model, a weakly compressible SPH model (Stansby *et al.* 2008) and (b) ISPH for solitary wave. The solitary wave has a height of 0.1 m and is generated in the SPH simulations using the Goring (1978) wavemaker. The agreement between the computed ISPH results and other numerical predictions results is close, but there are differences which will be the focus of future investigation.

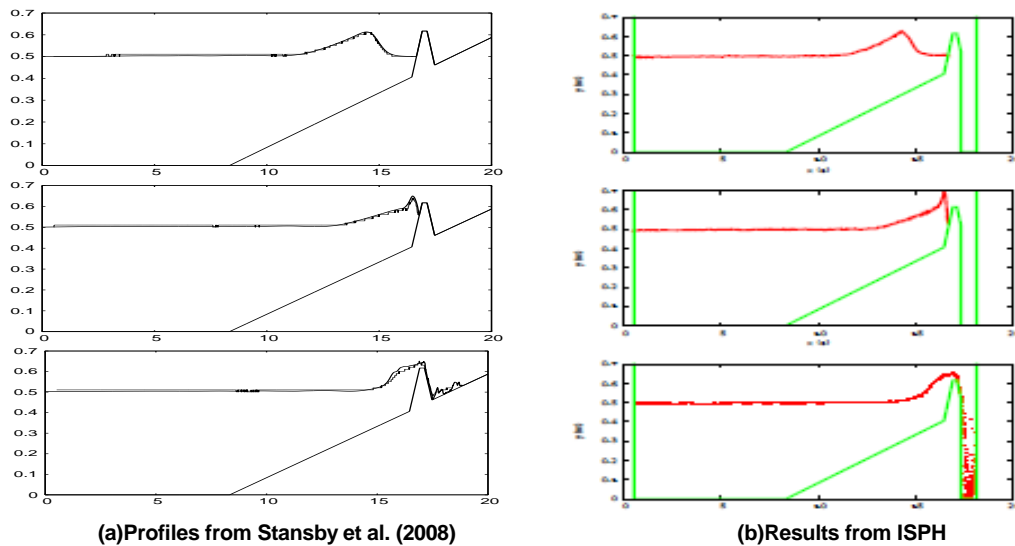


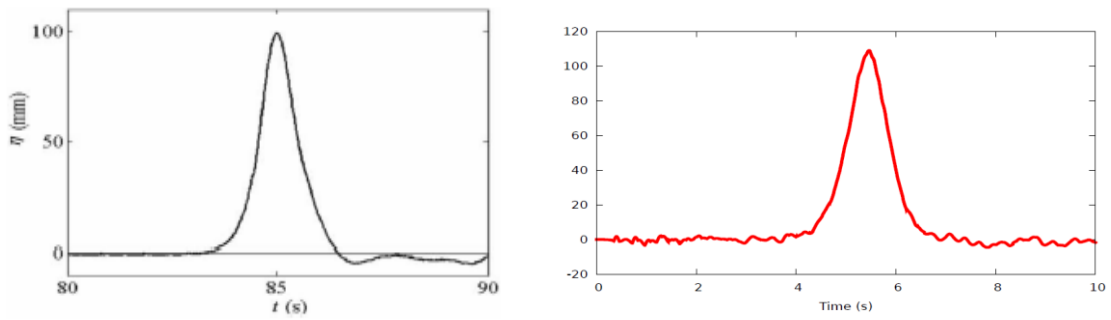
Figure 3 Surface profiles for a solitary wave at  $t = 8s$ ,  $t = 9s$ ,  $t = 10s$

Fig. 4 shows the time history of the free surface at the toe of the beach comparing the Boussinesq-type model of Stansby *et al.* (2008) with ISPH. The agreement of the peak elevation is reasonable with a difference of approximately 5% while the ISPH result predicts slightly more fluctuations.

Fig. 5 shows the water height of the overtopping flow at the seaward corner of the structure. The left-hand image displays the results reported by Stansby *et al.* (2008) for WCSPH, Boussinesq and experiments of Hunt Raby *et al.* (2011). The experiments of Hunt Raby *et al.* (2011) gave an overtopping height of approximately 0.06m. The ISPH results predict an overtopping height of

approximately 0.08 m while WCSPH results gave an overtopping height of 0.061 m and the Boussinesq results overpredict the height with 0.083 m. With such a violent process however, it is possible that the measurement of the overtopping height may contain unquantified variability requiring further investigation.

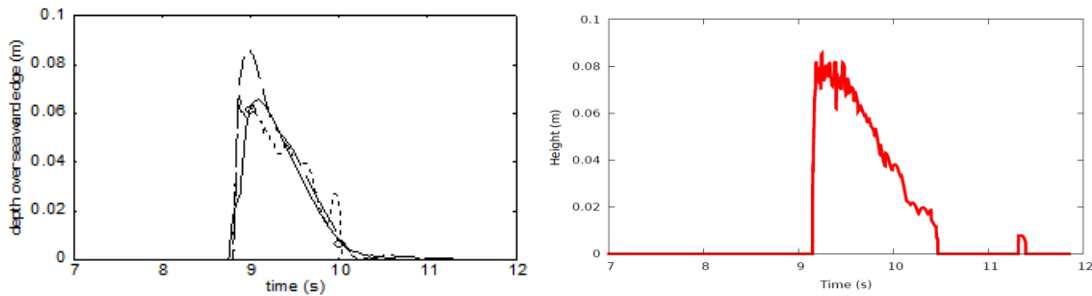
Fig. 6 shows a time history for the predicted overtopping volume. The ISPH results for the overtopping volume give 40 litres/m, which are in general agreement with the experimental value of 31 litres/m, but are overestimated for this low resolution. The agreement of ISPH with the experiment data is better than for a weakly compressible model, 20 litres/m for WCSPH at the same resolution (or particle size) of 0.01 m.



(a) Profiles from Stansby et al. (2008)

(b) Results from ISPH

Figure 4 Solitary wave free surface time histories at toe of beach



solid line (-): experiment, dashed line: (- -) Boussinesq scheme, dotted line: (...) WCSPH, diamonds: (◇) VOF

(a) Profiles from Stansby et al. (2008)

(b) Results from ISPH

Figure 5 Solitary wave overtopping water height

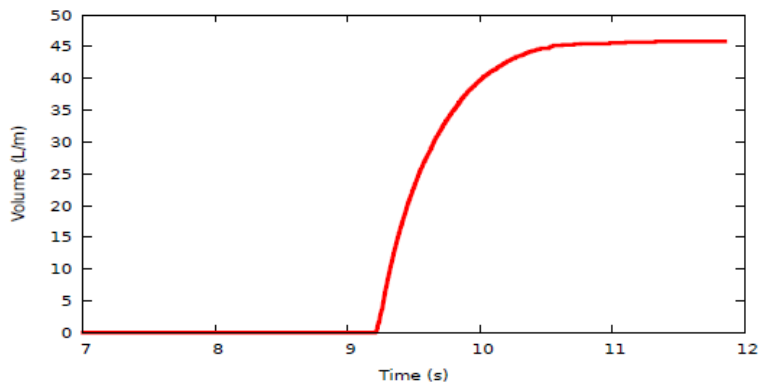


Figure 6 Overtopping history for ISPH for solitary wave

### Focussed Wave Group Overtopping

Hunt Raby *et al.* (2011) also conducted tests with focused wave groups. Herein, we present the results from ISPH for one of the cases where the wave was designed to come into focus immediately above the beach toe. The water level was measured at five wave gauges labelled in this paper as WG1 to WG5 as shown in Fig. 7.

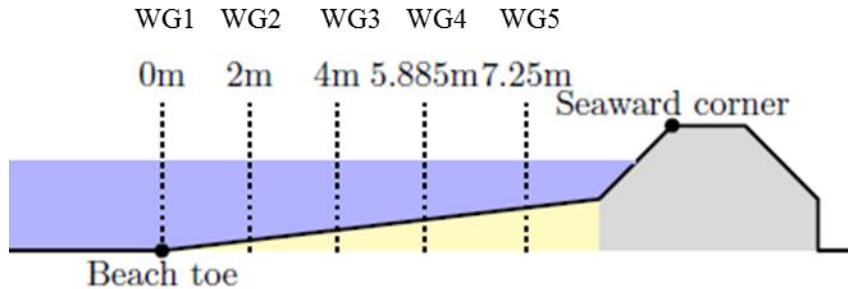


Figure 7 wave gauge location for focussed wave group overtopping

Fig. 8 shows a comparison of the measured free surface at each wave gauge and the free surface predicted by ISPH using the same resolution of 0.01 m (note that the vertical scales shown for the experimental and numerical results are not the same). The agreement is reasonable except when the focused wave group reaches WG5 which is located in the breaking region where the measurements will have included the aeration, where there is some oscillation evident in the ISPH results.

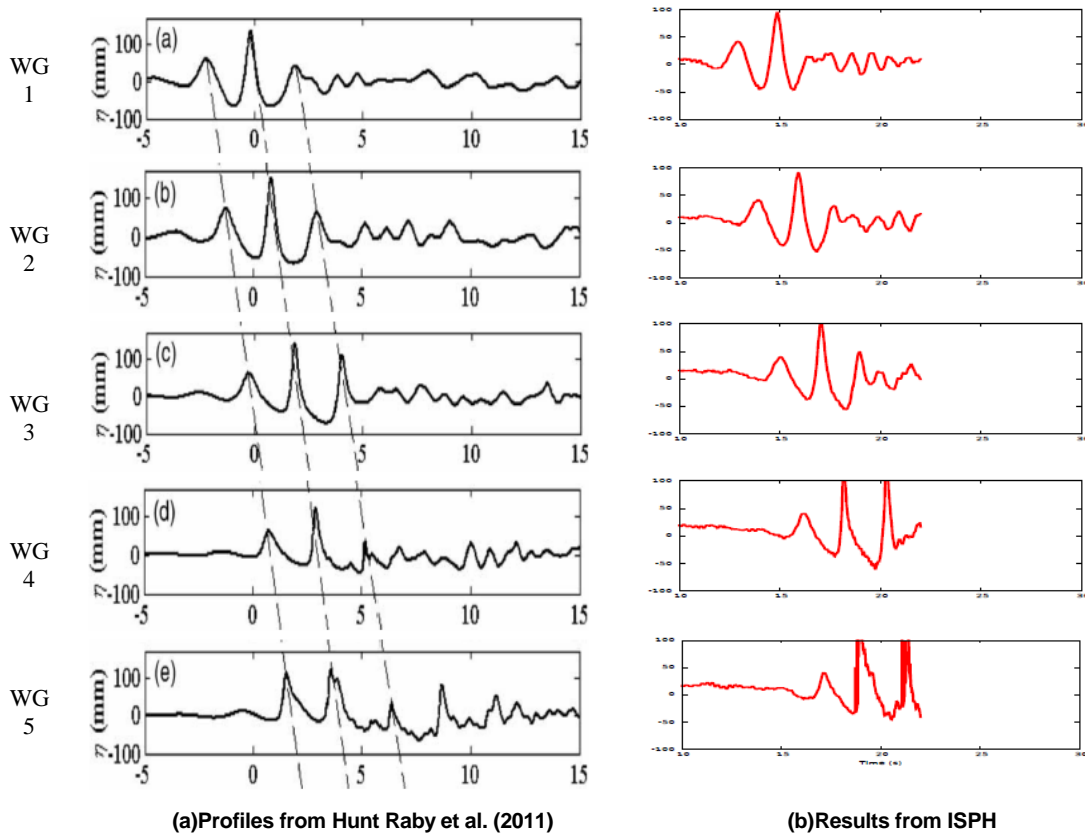


Figure 8 Focused wave group free-surface profiles at wave gauges WG1-5 (note: vertical axes are not on same scale, bottom axes represent time in seconds)

Finally, Fig. 9 shows the time history of the overtopping volume predicted by ISPH where there are two clear overtopping events in agreement with experimental observations and the final overtopping

volume predicted by ISPH is 9.8 litres/m compared to 12 litres/m measured in the experiments. The equivalent WCSPH scheme produced no overtopping whatsoever for this resolution.

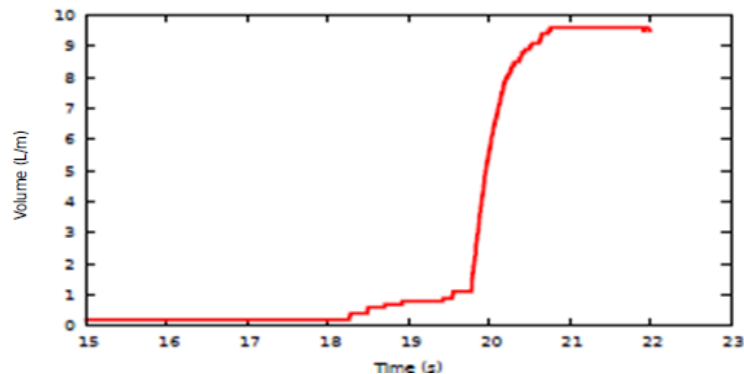


Figure 9 Overtopping volume history for focussed wave groups

### Discussion on boundary conditions

The ISPH simulations presented here used the multiple boundary tangent method (Yildiz *et al.* 2009). The results presented show satisfactory agreement with the experimental data of Hunt Raby *et al.* (2011), however, the simulations proved to be quite sensitive during development of this application, particularly when shifting was occurring near where the free surface meets a wall or boundary such as next to the paddle or the shallowest water. Boundary conditions have proven to be a difficult challenge in SPH as evidence by their identification as a Grand Challenge by the SPH European Research Interest Community (SPHERIC 2014). More recent developments could improve the robustness of the simulations, such as Ferrand *et al.* (2012) with the semi-analytical approach or Fourtakas *et al.* (2014) with a moving uniform stencil.

### CONCLUSIONS

This paper has presented the application of an incompressible SPH numerical scheme to the overtopping of breakwaters using the latest formulation improvements for ISPH including particle shifting. The paper has presented investigations into the modelling of different wave types including solitary waves and crest focussed wave groups looking at the hydrodynamics of the overtopping process in the vicinity of the obstacle with an improved ISPH formulation. The results for only one resolution (or particle size) have been presented but the results compare favourably with more established WCSPH models, and in the case of focussed wave group overtopping, the ISPH predicted overtopping in satisfactory agreement with the experimental data where the WCSPH scheme produced no overtopping whatsoever. In future work, more recent developments in solid wall boundary treatments will be introduced which will improve the robustness of the scheme.

### ACKNOWLEDGMENTS

The authors would like to thank EDF R&D for the financial support for the second author.

### REFERENCES

- Dalrymple, R.A. and Rogers, B.D., "Numerical Modeling of Water Waves with the SPH Method", *Coastal Engineering*, 53(2-3), 141-147, 2006.
- Cummins S.J., Rudman M., "An SPH projection method", *J. Comput. Phys.* 152, 584–607, 1999.
- Ferrand M, Laurence D R P, Rogers B D, Violeau D, Kassiotis C. "Unified semi-analytical wall boundary conditions for inviscid, laminar or turbulent flows in the meshless SPH method.". *International Journal for Numerical Methods in Fluids*. Vol. 71. Issue 4, 446-472, 2013.
- Fourtakas G., Dominguez J. M., Vacondio R., Nasar A., Rogers, B.D., "Local Uniform STencil (LUST) boundary conditions for 3-D irregular boundaries in DualSPHysics", *Proc. 9<sup>th</sup> Int. SPHERIC Workshop*, Paris, 103-110, 2014.

- Goring D.G., "Tsunamis – The propagation of long waves on a shelf", PhD thesis, California Institute of Technology, 1978.
- Hunt-Raby A., Borthwick A.G.L., Stansby P.K., Taylor P.H.. "Experimental measurement of focused wave group and solitary wave overtopping". *J. Hydraulic Research*, 49(4). 450-464, 2011.
- Lind S.J, Xu R, Stansby P.K, Rogers B.D. "Incompressible Smoothed Particle Hydrodynamics for Free-Surface flows: A Generalised Diffusion-Based Shifting for Stability and Validations for Impulsive Flows and Propagating Waves". *J. Comp. Phys.* 231(4), 1499-1523, 2012.
- Rogers, B.D., Dalrymple, R.A. and P.K. Stansby, "Simulation of Caisson Breakwater Movement using 2-D SPH", *J. Hydraulic Research*, Special Issue, 2010.
- Skillen A., Lind S.J., Stansby P.K., Rogers B.D. "Incompressible Smoothed Particle Hydrodynamics (SPH) with reduced temporal noise and generalised Fickian smoothing applied to body-water slam and efficient wave-body interaction". *Computer Methods in Applied Mechanics and Engineering*, 265, 163–173, 2013.
- SPHERIC, "SPHERIC Grand Challenge Working Group" [https://wiki.manchester.ac.uk/spheric/index.php/SPH\\_Theory\\_Working\\_Group](https://wiki.manchester.ac.uk/spheric/index.php/SPH_Theory_Working_Group), accessed 29 September 2014.
- Stansby P. K., Xu R., Rogers B.D., Hunt-Raby A., Borthwick A.G.L., Taylor P.H. "Modelling tsunami overtopping of a sea defence by shallow-water Boussinesq, VOF and SPH methods". *Proc. of Flood Risk Assessment Conference*, Oxford. September 2008.
- van der Vorst, H.A. "Bi-CGSTAB: a fast and smoothly converging variant of BI-CGSTAB for the solution of nonsymmetric linear systems", *SIAM J. Sci. Stat. Comput.* 13, 631-644, 1992.
- Xu R., Stansby P.K., Laurence D., Accuracy and stability in incompressible SPH (ISPH) based on the projection method and a new approach, *J. Comput. Phys.* 228, 6703–6725, 2009.
- Yildiz M., Rook R.A., Suleman A.. "SPH with the multiple boundary tangent method", *International Journal for Numerical Methods in Engineering*, 77(10), 1416-1438, 2009.